

# Optimization of railway microgrid operation under conditions of minimizing energy outflow to the grid

Piotr Obrycki, and Krzysztof Perlicki

**Abstract**—The railway energy microgrid, in terms of both photovoltaic installation and energy storage, should be dimensioned so that there is no or minimal energy outflow. Only under this assumption - that there is no energy flow outside the microgrid - can the consumer freely define the microgrid without the risk of disagreement from the grid operator. The article presents an optimization analysis of microgrid operation to minimize the energy exported to the grid. The microgrid operation was analysed regarding the load generated by one of Poland's railway traction substations. The Particle Swarm Optimization method was used to optimize microgrid operation. Different photovoltaic panel orientations, values for the maximum energy export, and depth of discharge of energy storage were considered. The results show that it is possible to significantly reduce the value of energy export to the grid and use excess energy to charge the designed optimal battery energy storage. An analysis of the green energy used to power the traction substation was also carried out. The results indicate that it can represent a significant percentage of the energy used to power a traction substation.

**Keywords**—photovoltaic; battery energy storage; railway microgrid; optimal design; Particle Swarm Optimization

## I. INTRODUCTION

THE railway is a transport mode that significantly contributes to policies promoting clean and sustainable transport. Even though its current technical and economic characteristics are superior to other modes of transport in terms of efficiency, there is growing interest in increasing its energy efficiency. Therefore, there is a great interest in the so-called intelligent management of railway systems in terms of rolling stock transport and its power supply. Two main challenges of smart management of railway systems can be mentioned. Firstly, railways consist of different subsystems of operation, infrastructure, and rolling stock, which should be integrated to ensure proper functioning. Secondly, smart management of the railway system implies a combination of multiple technologies, which increases the system's complexity and, thus, the difficulty of its effective implementation for operation [1]. Railway electricity systems have specific characteristics that distinguish them from other systems of this type. While the purpose of typical electricity systems is to provide electricity with well-defined characteristics, the primary purpose of railway systems is to provide timetabled passenger and freight transport. For this

reason, railway energy microgrids operate differently from conventional energy microgrids [2]. The main distinguishing feature of railway microgrids is that they are intended to provide, first of all, for the operation of train traffic with a well-defined spatio-temporal variability. Secondly, the energy consumption of individual trains can vary significantly. Thirdly, railway lines are often connected to several main electricity grids. In railway microgrids, there is a strong emphasis on reliable and secure broadband communication to guarantee the integration of distributed energy sources, energy storage systems, and intelligent energy management systems [3]. In the case of microgrids, the railway system operator is responsible for managing the distributed energy resources within the railway power system, i.e. energy storage and distributed energy sources. Managing the power flow between the railway microgrid and the main (distribution) power grid requires that traction substations are complemented by power subsystems capable of balancing energy in real-time [4]. The use of renewable energy sources (mainly photovoltaic) provides, in addition to the environmental aspects, significant energy savings by reducing energy consumption from the distribution network. However, the load on the traction line by passing trains and the renewable energy sources are characterized by strong stochastic variability; these characteristics are not correlated. The railway load varies over time and is often affected by various contingencies, and renewable energy generation is strongly affected by uncontrolled weather conditions [5], [6]. The solution to this problem is introducing an energy storage facility as a buffer for the railway energy system [7]. The management system in the railway energy microgrid must ultimately interact with the systems of the primary power grid. This approach aims to optimize the power demand profile while considering surplus and reduced local energy production by coordinating the operation of distributed energy sources and storage.

The main tasks of photovoltaic systems are to reduce the purchase of electricity and peak load demand. Photovoltaic systems can realize the reduction of electricity consumption at any time during their operation, but the reduction of peak demand is already more of a problem. This is because producing electricity by photovoltaic systems often does not coincide with peak demand hours. The solution to this problem is to use the

First Author: Piotr Obrycki is with Office of Research, Development and Aid Financing, PGE Energetyka Kolejowa S.A. (e-mail: Piotr.Obrycki@gkpge.pl).

Second Author: Krzysztof Perlicki is with Warsaw University of Technology (e-mail: krzysztof.perlicki@pw.edu.pl).



storage of excess energy produced during periods of low demand, with its use to meet peak demand. The main problem that arises here is to find the appropriate optimum size for photovoltaic installations and associated battery energy storage that can meet a specific energy demand with high probability. It becomes necessary to design the layout of the photovoltaic installation and energy storage to reduce the peak load on the electricity grid while considering its rather stochastic nature and the variable electricity production resulting from the variable nature of solar irradiance. Much attention is being paid to investigating the performance of a system consisting of photovoltaic installation and energy storage. Various methods and different objective functions can be found in the literature for solving the problem of techno-economic optimization of the performance of a photovoltaic installation-energy storage system. The most common methods include deterministic, stochastic, robust, and multi-objective optimization [8], [9], [10]. Many tools and mathematical methods are used to optimize the operation of systems consisting of photovoltaic installations and energy storage. These are divided into the following types: intuitive method, numerical method, analytical method, artificial intelligence, and hybrid methods [11], [12], [13]. In recent years, several studies have emerged on the problem of optimal sizing of a microgrid consisting of a photovoltaic installation and energy storage with different objectives and design variables. The analyses typically concern grid-connected households with a continuous energy consumption (load) pattern and repeatable maxima in the daily pattern. For example, work [14] proposed an optimal sizing method for a grid-connected photovoltaic installation-battery energy storage system, considering different electricity pricing tariffs to decrease the annual operation cost of the system. In work [15], an optimal sizing method for a grid-connected photovoltaic installation-battery energy storage system was proposed to minimize the consumer electricity bill. A techno-economic optimal approach was presented in [16] to minimize the total net present value of a household's photovoltaic installation-battery energy storage system considering the annual electricity consumption cost. A comprehensive method for the optimal design of a class of residential photovoltaic installation-battery energy storage microgrid was proposed in [17]. The optimization aimed to minimize the levelized cost of energy, which was limited by the annual total loss of the power supply and the operational constraints. In [18], the optimal sizing of photovoltaic installation and battery energy storage was investigated for a grid-connected household as well as a group of houses. This study was concerned with full charge/discharge capability for energy storage. Authors [19] present a multi-objective optimal sizing of the battery storage system and rooftop solar photovoltaic for a grid-connected household. The objective functions were selected as the cost of electricity and grid dependency. In [20], the size of the battery energy storage system was determined to supply energy to the load of auxiliary systems of an electric substation and a photovoltaic system to achieve a null total cost. Multi-objective optimization using the genetic algorithm technique was

employed to optimize the hybrid photovoltaic/battery energy storage system size to minimize the investment cost and time when the demand was unmet. Author [21] presents a technical and economic model for designing a grid-connected photovoltaic installation with a battery energy storage system, in which the electricity demand was satisfied through the photovoltaic-battery system and the national grid as the backup source. The aim was to present the photovoltaic-battery energy storage system design and management strategy and discuss the analytical model to determine the photovoltaic system rated power and the battery energy storage system capacity to minimize the levelized cost of the electricity. The study [22] presents a two-stage Adaptive Robust Optimization for optimal sizing and operation of residential photovoltaic systems coupled with battery units. The proposed model determined the optimal size of the photovoltaic - battery system while minimizing operating costs under the worst-case realization of uncertainties. There is a lack of a similar multi-threaded view of photovoltaic-battery systems for railway microgrids, their specific periodic load variations, and their high instantaneous load values. Moreover, previous analyses have not considered the constraint on the energy export from the railway energy microgrid to the grid and the analysis of the level of green energy used to power the traction substation. It is worth noting here, regarding the operation of microgrids in the railway system, several objectives can de facto be defined: to increase the share of photovoltaic installations in railway power supply, to improve the security of power supply to railway customers, or to increase the independence of the railway system from the National Electricity System. In each of these cases, it is important to limit the outflow of energy from photovoltaic installations operating within a microgrid outside the microgrid. First and foremost, renewables are dedicated to supplying local power and increasing the use of green energy locally. Thus, any energy export outside the microgrid, even with an equivalent energy intake from the National Electricity System, results in less energy from a photovoltaic installation dedicated to local supply. Furthermore, the microgrid, in terms of both photovoltaic installation and energy storage, should be dimensioned so that there is no or minimal energy export. Only under this assumption - that there is no energy flow outside the microgrid - can the consumer freely define the microgrid without the risk of disagreement from the grid operator. Thus, it is crucial to define algorithms and mechanisms that can limit energy export from the microgrid. Only then can the microgrid consumer be assured that renewables and energy storage are operating economically within an optimally designed microgrid. This paper analyses the energy balance of a railway microgrid with the objective function of minimizing the energy export to the grid. Hereinafter referred to as limited energy. It is assumed that the minimization of limited energy is associated with increased battery energy storage capacity. The minimization of limited energy and the associated increase in energy storage capacity are presented for different energy values produced by the photovoltaic installation. The Particle Swarm Optimization method was used to optimize microgrid operation. An analysis

of the green energy used to power a traction substation is also presented, understood as the ratio of the energy from the photovoltaic installation and the battery energy storage to the total energy consumed in the traction substation.

## II. MODELING OF RAILWAY MICROGRID

Figure 1 shows a diagram of the railway energy microgrid under study. The microgrid consists of a photovoltaic installation and battery energy storage. The photovoltaic installation is connected to the battery energy storage, the grid (distribution grid), and the traction substation. The photovoltaic installation first supplies the traction substation, further charges the battery energy storage, and the excess energy produced is exported to the grid. The energy export to the grid is assumed to be minimized starting from the assumed not-to-exceed energy surrendered. The battery energy storage capacity is assumed to be increased to ensure this assumption. A photovoltaic installation first supplies the traction substation. In an energy shortage, the energy storage facility is used, and next, the power supply comes from the grid.

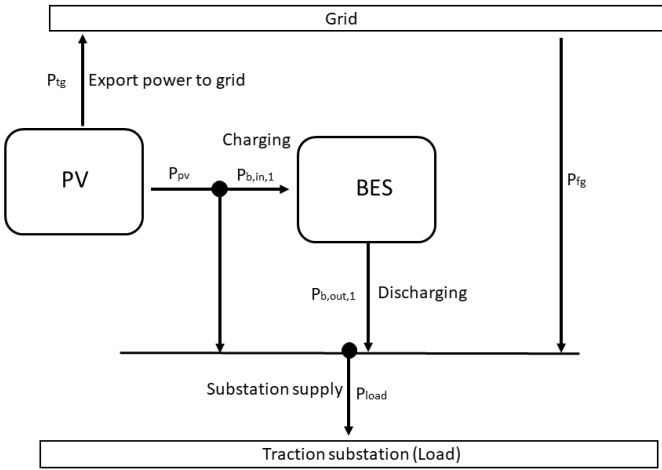


Fig. 1. Diagram of the analyzed railway microgrid; PV - photovoltaic installation, BES - battery energy storage,  $P_{pv}$  - power from photovoltaic,  $P_{b,in,1}$  - power associated with charging the energy storage,  $P_{b,out,1}$  - power associated with the discharge of the energy storage,  $P_{fg}$  - export power to grid,  $P_{fg}$  - import power from grid,  $P_{load}$  - load power

Figure 2 shows the decision algorithm as a block diagram for sizing the power export to the grid (limited energy), the size of battery energy storage depending on photovoltaic installation production and the load.

Meanwhile, Fig. 3 shows the selection rules used in the system under study. The following designations were used:  $P_{pv}$  - power from photovoltaic installation,  $P_{b,in,1}$  - power associated with charging the energy storage (power entering the storage),  $P_{b,out,1}$  - power associated with the discharge of the energy storage (power leaving the storage),  $P_{b,in,2}$  - available input power of battery energy storage,  $P_{b,out,2}$  - available output power of battery energy storage,  $P_{tg}$  - export power to grid,  $P_{fg}$  - import power from grid,  $P_{load}$  - load power.

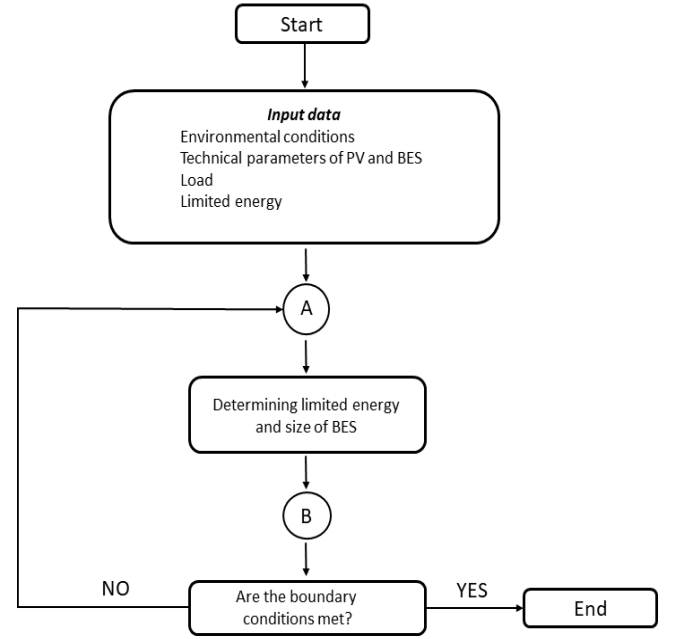


Fig. 2. Block diagram for determining the limited energy and size of battery energy storage depending on the photovoltaic installation size and load; PV – photovoltaic installation, BES – battery energy storage

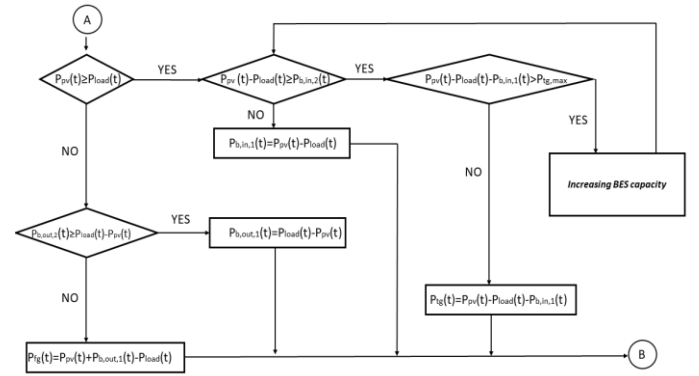


Fig. 3. Selection rules used to optimize the energy limited and size of battery energy storage depending on the photovoltaic installation size and load; BES – battery energy storage

In the adopted model, it was assumed that the effects of the sit total solar insolation  $N_{ac}$  [kW/m<sup>2</sup>] and the ambient temperature  $T_a$  [°C] are related to the output power of the photovoltaic module as follows [23]:

$$P_{pv}(t) = \eta_{pv} \cdot P_{r(pv)} \cdot \left(\frac{N_{ac}}{N_{stc}}\right) \cdot (1 - \gamma(T_{cell} - T_{stc})), \quad (1)$$

$$T_{cell} = T_a + \left(\frac{NOCT - 20^\circ C}{0.8 kW/m^2}\right) \cdot N_{ac}. \quad (2)$$

Where  $\eta_{pv}$  is photovoltaic module efficiency [%],  $P_{r(pv)}$  is rate unit power [kW],  $N_{stc}$  is insolation in Standard Test Conditions,  $\gamma$  is temperature derating [%/°C],  $T_{stc}$  is cell temperature in Standard Test Conditions [°C],  $NOCT$  is Normal Operating Cell Temperature [°C].

As already specified in our microgrid model, if the power produced by the photovoltaic installation exceeds the demand

from the traction substation in the form of a specific load, the energy storage will first be charged if its State Of Charge (SOC) allows it. The input power of the battery energy storage is within the accepted limits. Then, any additional electric power produced is sent to the grid. The value of this power is:

$$P_{tg}(t) = \min(P_{tg,max}, P_{pv}(t) - P_{load}(t) - P_{b,in,1}(t)). \quad (3)$$

If the power produced by the photovoltaic installation is less than the demand from the traction substation, battery energy storage discharging takes place, taking into account the SOC level of the battery energy storage and the boundary conditions of the power output from the battery energy storage. If the power from the photovoltaic installation is less than the demand from the traction substation, discharging the energy storage to meet the demand takes place first. This occurs when the level of the SOP, the output power, and the battery energy storage output power are within certain limits. Subsequently, the grid will provide any power shortfall. The import power from the grid is determined as follows:

$$P_{fg}(t) = P_{load}(t) - P_{pv}(t) - P_{b,out,1}(t). \quad (4)$$

The Depth Of Discharge (DOD) of the battery energy storage with State Of Charge (SOP) is related by the following relation  $DOD(t)=1-SOP(t)$ , where the following relationship can describe SOP [24]:

$$SOC(t + dt) = SOC(t) + \frac{P_{b,in,1}(t) \cdot \eta_{b,in} - P_{b,out,1}(t) / \eta_{b,out}}{Cos/h}, \quad (5)$$

where  $\eta_{b,in}$  is efficiency associated with charging battery energy storage,  $\eta_{b,out}$  is efficiency associated with discharging battery energy storage,  $CoS$  is Capacity of Storage,  $h$  is hour. The available input and output power of battery energy storage can be calculated as:

$$P_{b,in,2}(t) = \min\left(P_{b,max}, \left(\frac{Cos}{h}\right) \cdot (SOC_{max} - SOC(t))\right), \quad (6)$$

$$P_{b,out,2}(t) = \min\left(P_{b,max}, \left(\frac{Cos}{h}\right) \cdot (SOC(t) - SOC_{min})\right). \quad (7)$$

In addition, increasing battery energy storage capacity is proportional to  $P_{pv}(t) - P_{load}(t) - P_{tg}(t)$ .

### III. OPTIMIZATION MODEL

The objective function is to minimize the limited energy while maximizing the size of the battery energy storage for a given photovoltaic plant output and providing proper power to the traction substation. The method developed adopted the following boundary conditions limiting the obtained calculation results:

$$0 \leq P_{pv}(t) \leq P_{pv,max}, \quad (8)$$

$$P_{b,in,1}(t) \geq 0, \quad (9)$$

$$P_{b,out,1}(t) \leq P_{b,max}, \quad (10)$$

$$SOC_{min} \leq SOC(t) \leq SOC_{max}, \quad (11)$$

$$P_b(t) + P_{pv}(t) - P_{tg}(t) \geq P_{load}(t), \quad (12)$$

$$P_{tg}(t) \leq P_{tg,max}. \quad (13)$$

Relationship (8) relates to the power limitation of the photovoltaic system, and relationships (9) and (10) describe limitations on the operation of the battery energy storage. Relation (11) represents constraints related to the state of charge/discharge of the battery energy storage. Relationship (12) shows the constraint for power balance at each time. Relationship (13) is the grid constraint to limit the export power from the photovoltaic installation to the grid. Relationship (13) relates to limited energy.

The Particle Swarm Optimization (PSO algorithm) method is one of the most widely used. This method works well in practice and can be easily adapted to solve almost any problem, regardless of the form of the objective function, imposed constraints, or the solution space size. This algorithm has successfully solved power system optimization problems [25]. The Particle Swarm algorithm is well-known among evolutionary algorithms due to its appropriate convergence rate, simplicity, and minimal dependence on initial points [26]. The particle swarm optimization algorithm was developed by James Kennedy and Russell C. Eberhart [27]. The algorithm is based on a description of the behaviour of a population of particles in which there is communication between particles and information sharing, with each particle having a specific position and speed. The particles move to new positions, searching for the optimum, and change direction if a better solution is found. Each particle knows its neighbours and remembers its best positions and the position of its neighbours. The optimization process is implemented iteratively and boils down to finding successively better positions of particles in the search space and in the final finding of the best solution in the form of the best position to which the whole group of particles, or swarm, converges. During the optimization process, the position of each particle is determined by its previous experience and that of the entire group. A swarm consists of  $n$  particles. A single particle is described by a position  $x_i$ , representing a potential solution, and a velocity  $v_i$ , which determines the direction and distance over which the particle can move. At iteration  $k$  of the algorithm, a new position of particle  $i$  is determined using the relation [28, 29]:

$$x_i^k = x_i^{k-1} + v_i^k, \quad i=1, \dots, n, \quad (14)$$

where  $x_i^{k-1}$  is the position of the particle in the previous iteration,  $v_i^k$  is the velocity of the particle determined from its previous velocity  $v_i^{k-1}$ , the best position so far  $p_i$  and the position of the best particle in the swarm  $g$  according to the formula:

$$v_i^k = w \cdot v_i^{k-1} + c_1 \cdot r_1 \cdot (p_i - x_i^{k-1}) + c_2 \cdot r_2 \cdot (g - x_i^{k-1}), \quad i=1, \dots, n. \quad (15)$$

The parameter  $w$ , the inertia weight of the particle's motion, affects its ability to retain its previous velocity. As the value of  $w$  increases, the particle's ability to search new regions of the solution space increases. The parameter  $c_1$  is the cognition weight, which expresses a particle's confidence level. With this parameter, the intensity of searching local areas near the best positions of individual particles is controlled. The parameter  $c_2$  is the social weight and expresses a given particle's confidence level in the swarm's best particle. The  $c_2$  parameter controls the rate of following the currently best global solution. Meanwhile,  $r_1$  and  $r_2$  are random numbers in the interval  $[0, 1]$ .

The particle swarm optimization algorithm worked according to the following scheme:

- 1 Set the initial values of the parameters  $w$ ,  $c_1$ ,  $c_2$ .
2. setting  $k=0$ . generating the initial swarm  $R(k)$ .
3. For each particle  $i$  in  $R(k)$ , determine the objective function.
4. Remembering the best particle  $g$  in  $R(k)$ . For each particle  $i$  in  $R(k)$ , memorize its current position as the best  $p_i$ .
5. As long as the boundary conditions are not satisfied, perform:
  - (a) set  $k=k+1$ ,
  - (b) generate a new swarm  $R(k)$  based on  $R(k-1)$  using (14) and (15),
  - (c) for each particle  $i$  in  $R(k)$  determine the value of the objective function,
  - (d) for each particle  $i$  in  $R(k)$  updating its best position  $p_i$ ,
  - (e) updating the best position  $g$  in the entire  $R(k)$  swarm.
6. Returning the best solution  $g$  found.

In the particle swarm algorithm, the computational process is repeated for each generation until the algorithm is terminated when the maximum number of generations is reached. Thus, the best-repeated solution is selected as the optimal one. The following values were assumed in the calculations: population=50, generations=100, inertia weight  $w=0.5$ , cognition weight  $c_1=2$ , and social weight  $c_2=2$ . The PSO algorithm was done in 10 runs to achieve the global optimal results for the system under analysis.

## IV. RESULTS

### A. Input data

Input data include environmental conditions affecting the operation of the photovoltaic installation, technical parameters of the photovoltaic installation and battery energy storage, and load on the traction substation and limit energy.

#### 1) Environmental conditions

The calculation was carried out for data on the Garbce Zmigrod traction substation (51°30'47"N 16°53'03"E). Solar irradiation (Fig. 4a) and temperature (Fig. 4b) data for 2007 were used to analyse the operation of the photovoltaic installation. The data were taken from [30].

The 2007 figures are statistically closest to the median for 2005-2020. Two orientations for the location of the photovoltaic

panels were considered in the calculations, i.e. a south orientation and an east-west orientation.

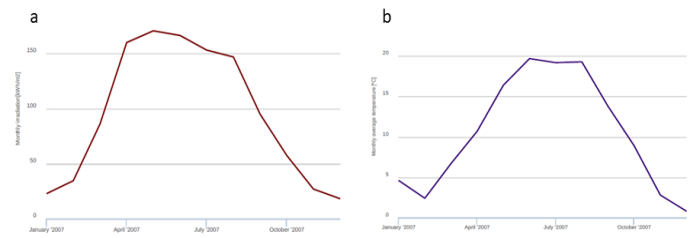


Fig. 4. Monthly irradiation (a) and average monthly temperature (b) for the analyzed traction substation (Garbce Zmigrod) location

### 2) Technical parameters

#### Photovoltaic installation:

- photovoltaic module efficiency ( $\eta_{pv}$ ): 90 %
- rate unit power ( $P_{r(pv)}$ ): 10 kW
- insolation in Standard Test Conditions ( $N_{stc}$ ): 1 kW/m<sup>2</sup>
- temperature derating ( $\gamma$ ): 0.5 % W/°C
- cell temperature in Standard Test Conditions ( $T_{stc}$ ): 25 °C
- Normal Operating Cell Temperature (NOCT): 45 °C

#### Battery energy storage:

- efficiency associated with charging battery energy storage ( $\eta_{b,in}$ ): 90 %
- efficiency associated with discharging battery energy storage ( $\eta_{b,out}$ ): 90 %
- maximum DOD ( $DOD_{max}$ ): 50 % and 80 %.
- initial SOC: 75 %
- maximum SOC ( $SOC_{max}$ ): 100 %.
- minimum SOC ( $SOC_{min}$ ): 50 % and 20 %.

### 3) Load on the traction substation

The calculations included the traction substation electricity load data from the central repository for measurement data of the PGE Energetyka Kolejowa (Polish Railway Power Company). The results of the substation under analysis for the entire year 2023 were used. Figure 5 shows an example of daily load changes of the analyzed traction substation (Garbce Zmigrod) and load histogram for the year 2023.

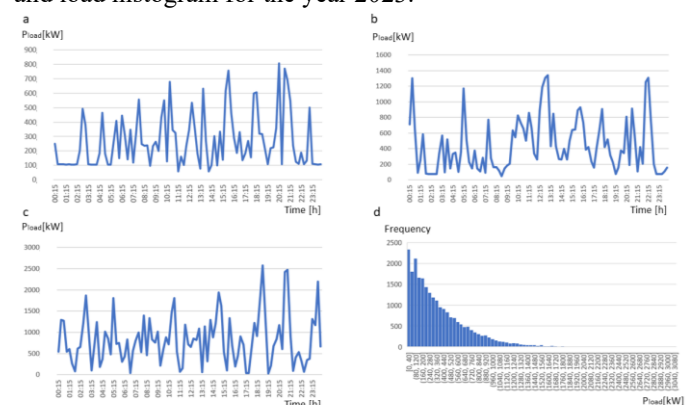


Fig. 5. Daily load changes (a-c) and load histogram (d) for the year 2023 (Garbce Zmigrod traction substation); for particularly marked value intervals, the load with values above 1.8 MW occurred no more than 5 times in a given interval

#### 4) Limited energy

The limited energy condition is described by the associated electrical power in the form of (13). In the system under analysis, minimizing the energy export to the grid was taken as the objective function. During the calculations, a maximum value for limited energy of 5 % and 20 % of the energy produced by the photovoltaic installation was assumed. These values are also the starting values in the optimization process. Minimizing the limited energy comes at the expense of increasing energy storage capacity.

#### B. Simulation results

Tables I-IV include the minimum value of energy limited ( $E_{TG,MIN}$ ) and the capacity of battery energy storage (CoS) at a given value of the photovoltaic installation ( $P_{PV}$ ). The value of the energy generated by the photovoltaic installation in one full year is also given ( $TE_{PV}$ ). Example simulation results are presented.

TABLE I

MINIMUM VALUE OF ENERGY LIMITED ( $E_{TG,MIN}$ ) AND THE CAPACITY OF BATTERY ENERGY STORAGE (CoS) AT A GIVEN VALUE OF THE PHOTOVOLTAIC INSTALLATION ( $P_{PV}$ ) AND THE ANNUAL VALUE OF THE ENERGY GENERATED BY THE PHOTOVOLTAIC INSTALLATION ( $TE_{PV}$ ); SOUTH ORIENTATION PHOTOVOLTAIC INSTALLATION, DOD=80%, MAXIMUM VALUE OF LIMITED ENERGY 5%

$P_{PV}$ [kW]	$TE_{PV}$ [MWh]	$E_{TG,MIN}$ [kWh]	CoS [kWh]
20	20.90	0.19	134
40	41.80	0.02	1275
60	62.70	0.07	8728
80	83.59	0.00	17640
100	104.49	0.00	27367
120	125.39	0.00	38908
140	146.29	0.00	50588
160	167.19	0.68	62303

TABLE II

MINIMUM VALUE OF ENERGY LIMITED ( $E_{TG,MIN}$ ) AND THE CAPACITY OF BATTERY ENERGY STORAGE (CoS) AT A GIVEN VALUE OF THE PHOTOVOLTAIC INSTALLATION ( $P_{PV}$ ) AND THE ANNUAL VALUE OF THE ENERGY GENERATED BY THE PHOTOVOLTAIC INSTALLATION ( $TE_{PV}$ ); SOUTH ORIENTATION PHOTOVOLTAIC INSTALLATION, DOD=50%, MAXIMUM VALUE OF LIMITED ENERGY 5%

$P_{PV}$ [kW]	$TE_{PV}$ [MWh]	$E_{TG,MIN}$ [kWh]	CoS [kWh]
20	20.90	0.00	215
40	41.80	0.02	2040
60	62.70	0.00	13965
80	83.59	0.00	28224
100	104.49	0.81	43785
120	125.39	0.83	62250
140	146.29	1.28	80937
160	167.19	2.77	99683

TABLE III

MINIMUM VALUE OF ENERGY LIMITED ( $E_{TG,MIN}$ ) AND THE CAPACITY OF BATTERY ENERGY STORAGE (CoS) AT A GIVEN VALUE OF THE PHOTOVOLTAIC INSTALLATION ( $P_{PV}$ ) AND THE ANNUAL VALUE OF THE ENERGY GENERATED BY THE PHOTOVOLTAIC INSTALLATION ( $TE_{PV}$ ); SOUTH ORIENTATION PHOTOVOLTAIC INSTALLATION, DOD=80%, MAXIMUM VALUE OF LIMITED ENERGY 20%

$P_{PV}$ [kW]	$TE_{PV}$ [MWh]	$E_{TG,MIN}$ [kWh]	CoS [kWh]
20	16.60	0.05	111
40	33.19	0.00	307
60	49.79	0.00	4194
80	66.39	0.14	11515
100	82.98	0.00	19142
120	99.58	0.00	29021
140	116.18	0.51	49020
160	132.78	0.96	69312

Table IV

MINIMUM VALUE OF ENERGY LIMITED ( $E_{TG,MIN}$ ) AND THE CAPACITY OF BATTERY ENERGY STORAGE (CoS) AT A GIVEN VALUE OF THE PHOTOVOLTAIC INSTALLATION ( $P_{PV}$ ) AND THE ANNUAL VALUE OF THE ENERGY GENERATED BY THE PHOTOVOLTAIC INSTALLATION ( $TE_{PV}$ ); EAST-WEST ORIENTATION PHOTOVOLTAIC INSTALLATION, DOD=80%, MAXIMUM VALUE OF LIMITED ENERGY 5%

$P_{PV}$ [kW]	$TE_{PV}$ [MWh]	$E_{TG,MIN}$ [kWh]	CoS [kWh]
20	20.90	0.19	134
40	41.80	0.02	1275
60	62.70	0.07	8728
80	83.59	0.00	17640
100	104.49	0.00	27367
120	125.39	0.00	38908
140	146.29	0.00	50588
160	167.19	0.68	62303

The results obtained (Tab. I-IV) indicate that the limited energy can be significantly reduced relative to the assumed maximum value with the proposed optimization method. The reduction in limited energy is accompanied by an increase in the battery energy storage capacity to store the excess energy that occurs. The same results were obtained for the minimum limited energy with a different value for the maximum value of limited energy from which the optimisation process was started (Tab. I and Tab. III). Moreover, the results indicate that it is possible, in some cases, to achieve a situation where limited energy produced is not sent to the distribution grid. This is the situation for  $P_{PV}=20$  kW (Tab. II), 40 kW (Tab. IV), 60 kW (Tab. II, Tab. IV), 80 kW (Tab. I, Tab. II, Tab. III), 100 kW (Tab. I, Tab. III, Tab. IV), 120 kW (Tab. I, Tab. III, Tab. IV), 140 kW (Tab. I, Tab. III). In the analysed railway energy microgrid, the energy consumed by the traction substation first comes from the photovoltaic installation, then from battery energy storage, and

finally from the grid. An important parameter characterizing the operation of the analysed railway microgrid is green energy. This parameter is defined as the energy ratio from the photovoltaic installation to the total energy consumed in the traction substation. Energy from a photovoltaic installation can come directly from it as well as from battery energy storage. Figure 6 shows the relationship between green energy (GE) and the photovoltaic installation ( $P_{pv}$ ) value for a south orientation of photovoltaic panels.

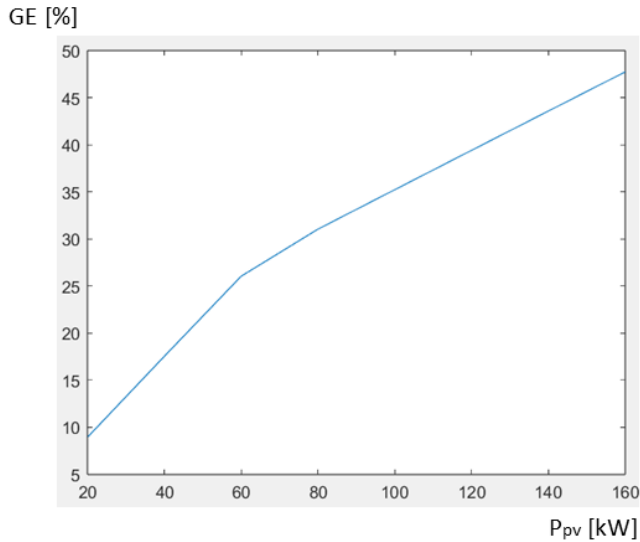


Fig. 6. Dependence of green energy level (GE) on the value of the photovoltaic installation ( $P_{pv}$ ) for a south orientation of photovoltaic panels

The results shown in Fig.6 indicate that green energy levels can range from a few percent to 48 percent, with a strong dependence on the production value of the photovoltaic installation. Figure 7 shows the evolution of the limited energy optimization process and the accompanying process of increasing the battery energy storage capacity and the green energy in the traction substation supply. Results were obtained for: south orientation photovoltaic installation, DOD = 80%, the maximum value of limited energy 5 %, the value of the photovoltaic installation 20 kW, and the annual value of energy generated by the photovoltaic installation 20.90 MWh.

The results in Fig.7 show that it is possible to select the size of the limited energy and the size of the battery energy storage capacity as required. It is possible to stop minimizing the limited energy by considering a specific battery energy storage capacity value. For example, for south orientation photovoltaic installation, DOD = 50%, the maximum value of limited energy 5 % and  $P_{pv}=40$ kW the following values are obtained in the process of minimizing limited energy (Tab. V). For the case with Tab. V, the minimum value of  $E_{lg}$  reaches zero. Associated with this is  $CoS=2040$  kWh. This is a large value for the energy storage capacity. For practical reasons, a storage with a capacity of 1077 kWh can be chosen. Such storage capacities

are often installed in national railway microgrids. With such a storage capacity, we also have limited energy at a very low level.

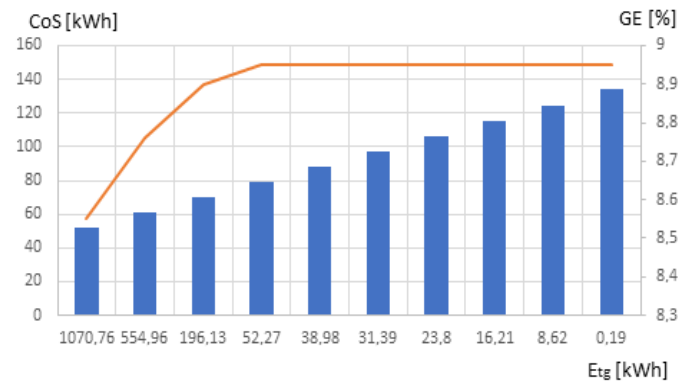


Fig. 7. Evolution of the limited energy ( $E_{lg}$ ) optimization process and the accompanying process of increasing the battery energy storage CoS (bars) and the green energy GE (continuous line)

TABLE V  
SELECTED VALUES OBTAINED BY VALUE OF ENERGY LIMITED ( $E_{TG}$ ) AND THE CAPACITY OF BATTERY ENERGY STORAGE ( $CoS$ ) DURING THE OPTIMISATION PROCESS

$E_{TG}$ [kWh]	$E_{TG}$ [%]	$CoS$ [kWh]
2106.69	5.00	308
889.52	2.14	692
507.56	1.22	1077
304.65	0.73	1462
101.74	0.24	1847
0.00	0.00	2040

## CONCLUSION

The conducted study underlined the application of the Particle Swarm Optimization approach in determining the limited energy and the associated optimization of battery energy storage size and green energy level. The optimization of the minimum energy value sent to the grid and the associated process of maximizing the battery energy storage capacity value are presented. Different photovoltaic panel orientations, values for the maximum limited energy level, and depth of discharge were considered. The method presented can be used at the design stage of a railway microgrid, which consists of photovoltaic installation and battery energy storage. With a given size of the photovoltaic installation and a known load pattern of the traction station, the presented method allows minimization of energy export to the grid, i.e. limited energy. The results show that it is possible to significantly reduce the value of limited energy and use excess energy to charge the designed optimal battery energy storage. The theoretical values of the battery energy storage capacity obtained are very large in many cases. However, it



must be remembered that these are the maximum values.

Minimizing the limited energy can be stopped at a higher value due to the practical sense of the obtained value of the battery energy storage capacity. The green energy values obtained indicate that the share of energy produced by a photovoltaic installation can meet the demand of a traction station from a single percentage to a very high level, close to 50 % in some cases.

## REFERENCES

- [1] E -LOBSTER Electric losses balancing through integrated storage and power electronics towards increased synergy between railways and electricity distribution networks, H2020-LCE-2016-2017, European Commission, Innovation and Networks Executive Agency, Grant agreement no. 731249, Deliverable D1.8, Smart Management of Railway Networks, 2020
- [2] E. Pilo de la Fuente, S. K. Mazumder and I. G. Franco, "Railway Electrical Smart Grids: An introduction to next-generation railway power systems and their operation," *IEEE Electrification Magazine*, vol. 2, no. 3, pp. 49-55, 2014. <https://doi.org/10.1109/MELE.2014.2338411>
- [3] Z. Kljaic, D. Pavkovic, M. Cipek, M. Trstenjak, T. J. Mlinaric, M. Niksic, "An Overview of Current Challenges and Emerging Technologies to Facilitate Increased Energy Efficiency," *Safety, and Sustainability of Railway Transport, Future Internet*, vol. 15, no. 11, pp. 347-391, 2023. <https://doi.org/10.3390/fi15110347>
- [4] M. Brenna, F. Foiadelli and H. J. Kaleybar, "The Evolution of Railway Power Supply Systems Toward Smart Microgrids: The concept of the energy hub and integration of distributed energy resources," *IEEE Electrification Magazine*, vol. 8, no. 1, pp. 12-23, 2020. <https://doi.org/10.1109/MELE.2019.2962886>
- [5] H. Hayashiya, Y. Watanabe, Y. Fukasawa, T. Miyagawa, A. Egami, "Cost impacts of high efficiency power supply technologies in railway power supply - Traction and Station -,", 2012 15th International Power Electronics and Motion Control Conference (EPE/PEMC), Novi Sad, Serbia, pp. LS3e.4-1-LS3e.4-6, 2012. <https://doi.org/10.1109/EPEPEMC.2012.6397441>
- [6] H. Hayashiya, H. Yoshizumi, T. Suzuki, T. Furukawa, T. Kondoh, "Necessity and possibility of smart grid technology application on railway power supply system," *Proceedings of the 2011 14th European Conference on Power Electronics and Applications*, Birmingham, UK, pp. 1-10, 2011.
- [7] F. Ma, X. Wang, L. Deng, Z. Zhu, Q. Xu and N. Xie, "Multiport Railway Power Conditioner and Its Management Control Strategy With Renewable Energy Access," *IEEE Journal of Emerging and Selected Topics in Power Electronics*, vol. 8, no. 2, pp. 1405-1418, 2020. <https://doi.org/10.1109/JESTPE.2019.2899138>
- [8] R. Nematirad, A. Pahwa, B. Natarajan, H. Wu, "Optimal sizing of photovoltaic-battery system for peak demand reduction using statistical models," *Frontiers in Energy Research*, paper number 11:1297356, 2023. <https://doi.org/10.3389/fenrg.2023.1297356>
- [9] C. O. Okoye, O. Solyali, "Optimal sizing of stand-alone photovoltaic systems in residential buildings," *Energy*, vol. 126, pp. 573-584, 2017. <https://doi.org/10.1016/j.energy.2017.03.032>
- [10] R. Belfkira, L. Zhang, G. Barakat, "Optimal sizing study of hybrid wind/PV/diesel power generation unit," *Solar Energy*, vol. 85, no. 1, pp. 100-110, 2011. <https://doi.org/10.1016/j.solener.2010.10.018>
- [11] S. Mandelli, C. Brivio, E. Colombo, M. Merlo, "A sizing methodology based on Levelized Cost of Supplied and Lost Energy for off-grid rural electrification systems," *Renewable Energy*, vol. 89, pp. 475-488, 2016. <https://doi.org/10.1016/j.renene.2015.12.032>
- [12] C. B. Salah, K. Lamamra, A. Fatnassi, "New optimally technical sizing procedure of domestic photovoltaic panel/battery system," *Journal of Renewable and Sustainable Energy*, vol. 7, paper number 013134, 2015. <https://doi.org/10.1063/1.4907923>
- [13] A. Mellit, "ANN-based GA for generating the sizing curve of stand-alone photovoltaic systems," *Advances in Engineering Software*, vol. 41, no. 5, pp. 687-693, 2010. <https://doi.org/10.1016/j.advengsoft.2009.12.008>
- [14] L. Zhou, Y. Zhang, X. Lin, C. Li, Z. Cai, and P. Yang, "Optimal sizing of PV and BESS for a smart household considering different price mechanisms," *IEEE Access*, vol. 6, pp. 41 050–41 059, 2018.
- [15] R. Khalilpour, A. Vassallo, "Planning and operation scheduling of pv-battery systems: A novel methodology," *Renewable and Sustainable Energy Reviews*, vol. 53, pp. 194–208, 2016. <https://doi.org/10.1016/j.rser.2015.08.015>
- [16] O. Erdinc, N. G. Paterakis, I. N. Pappi, A. G. Bakirtzis, and J. P. Catalao, "A new perspective for sizing of distributed generation and energy storage for smart households under demand response," *Applied Energy*, vol. 143, pp. 26–37, 2015. <https://doi.org/10.1016/j.apenergy.2015.01.025>
- [17] M. Alramlawi, P. Li, "Design Optimization of a Residential PV-Battery Microgrid With a Detailed Battery Lifetime Estimation Model," *IEEE Transactions on Industry Applications*, vol. 56, no. 2, pp. 2020-2030, 2020. <https://doi.org/10.1109/TIA.2020.2965894>
- [18] J. Li, "Optimal sizing of grid-connected photovoltaic battery systems for residential houses in Australia," *Renewable Energy*, vol. 136, pp. 1245–1254, 2019. <https://doi.org/10.1016/j.renene.2018.09.099>
- [19] R. Khezri, A. Mahmoudi and H. Aki, "Multi-Objective Optimization of Solar PV and Battery Storage System for A Grid-Connected Household," 2020 IEEE International Conference on Power Electronics, Drives and Energy Systems (PEDES), pp. 1-6, Jaipur, India, 2020. <https://doi.org/10.1109/PEDES49360.2020.9379481>
- [20] A. Gonçalves, G. O. Cavalcanti, M. A. F. Feitosa, R. F. D. Filho, A. C. Pereira, E. B. Jatoba, J. B. de Melo Filho, M. H. N. Marinho, A. Converti, L. A. Gómez-Malagon, "Optimal Sizing of a Photovoltaic/Battery Energy Storage System to Supply Electric Substation Auxiliary Systems under Contingency," *Energies*, vol. 16, no. 13, paper number 5165, 2023. <https://doi.org/10.3390/en16135165>
- [21] M. Bortolini, M. Gamberi, A. Graziani, "Technical and economic design of photovoltaic and battery energy storage system," *Energy Conversion and Management*, vol. 86, pp. 81-92, 2014. <https://doi.org/10.1016/j.enconman.2014.04.089>
- [22] M. Aghamohamadi, A. Mahmoudi, M. H. Haque, "Two-Stage Robust Sizing and Operation Co-Optimization for Residential PV–Battery Systems Considering the Uncertainty of PV Generation and Load," *IEEE Transactions on Industrial Informatics*, vol. 17, no. 2, pp. 1005-1017, 2021. <https://doi.org/10.1109/TII.2020.2990682>
- [23] G. M. Masters, K. F. Hsu, "Renewable and Efficient Electric Power Systems," 3rd Edition, John Wiley & Sons, Inc. – IEEE Press, USA, pp. 331-388, 2023
- [24] R. Khezri, A. Mahmoudi, M. H. Haque, "Optimal Capacity of Solar PV and Battery Storage for Australian Grid-Connected Households," *IEEE Transactions on Industry Applications*, vol. 56, no. 5, pp. 5319-5329, 2020. <https://doi.org/10.1109/TIA.2020.2998668>



- [25] Y. del Valle, G. K. Venayagamoorthy, S. Mohagheghi, J. C. Hernandez and R. G. Harley, "Particle Swarm Optimization: Basic Concepts, Variants and Applications in Power Systems," *IEEE Transactions on Evolutionary Computation*, vol. 12, no. 2, pp. 171-195, 2008. <https://doi.org/10.1109/TEVC.2007.896686>
- [26] M. Combe, A. Mahmoudi, M.H. Haque, R. Khezri, "Optimal sizing of an AC-coupled hybrid power system considering incentive-based demand response," *IET Generation, Transmission & Distribution*, vol. 13, no. 15, pp. 3354–3361, 2019. <https://doi.org/10.1049/iet-gtd.2018.7055>
- [27] J. Kennedy, R. Eberhart, "Particle swarm optimization," *Proceedings of ICNN'95 - International Conference on Neural Networks*, Perth, WA, Australia, Vol. 4, pp. 1942-1948, 1995. <https://doi.org/10.1109/ICNN.1995.488968>
- [28] Y. Shi, R. Eberhart, "A modified particle swarm optimizer," 1998 *IEEE International Conference on Evolutionary Computation Proceedings. IEEE World Congress on Computational Intelligence (Cat. No.98TH8360)*, Anchorage, AK, USA, pp. 69-73, 1998. <https://doi.org/10.1109/ICEC.1998.699146>
- [29] H. Hajian-Hoseinabadi, S. H. Hosseini, M. Hajian, "Optimal power flow solution by a modified particle swarm optimization algorithm," *2008 43rd International Universities Power Engineering Conference*, Padova, Italy, pp. 1-4, 2008. <https://doi.org/10.1109/UPEC.2008.4651443>
- [30] PVGIS.COM Photovoltaic Geographical Information System, <https://pvgis.com>